HHS Public Access

Author manuscript

J Immunol. Author manuscript; available in PMC 2022 April 01.

Published in final edited form as:

J Immunol. 2021 April 01; 206(7): 1505–1514. doi:10.4049/jimmunol.1901464.

A point mutation in IKAROS ZF1 causes a B cell deficiency in mice

Brigette Boast[*,1], **Lisa A. Miosge**[*,1], **Hye Sun Kuehn**[†], **Vicky Cho**[*], **Vicki Athanasopoulos**[*,‡], **Hayley A. McNamara**[*], **Yovina Sontani**[*], **Yan Mei**[*], **Debbie Howard**[*], **Henry J. Sutton**[*], **Sofia A. Omari**[*], **Zhijia Yu**[*], **Mariam Nasreen**[§], **T. Daniel Andrews**[*], **Ian A. Cockburn**[*], **Christopher C. Goodnow**[¶], **Sergio D. Rosenzweig**[†], **Anselm Enders**[*]

[*]Department of Immunology and Infectious Disease, John Curtin School of Medical Research, The Australian National University, ACT, Australia

[†]Immunology Service, Department of Laboratory Medicine, National Institutes of Health Clinical Center, MD, The United States of America

[‡]Centre for Personalised Immunology (NHMRC Centre for Research Excellence), John Curtin School of Medical Research, The Australian National University, ACT, Australia

[§]Australian Phenomics Facility, John Curtin School of Medical Research, The Australian National University, ACT, Australia

[¶]Immunology Division, Garvan Institute of Medical Research, NSW, Australia

Abstract

IKZF1 (IKAROS) is essential for normal lymphopoiesis in both humans and mice. Previous *Ikzf1* mouse models have demonstrated the dual role for IKZF1 in both B and T cell development and have indicated differential requirements of each zinc finger. Furthermore, mutations in *IKZF1* are known to cause common variable immunodeficiency (CVID) in patients characterized by a loss of B cells and reduced antibody production. Through ENU mutagenesis, we have discovered a novel *Ikzf1* mutant mouse with a missense mutation (L132P) in zinc finger 1 (ZF1) located in the DNA binding domain. Unlike other previously reported murine *Ikzf1* mutations, this L132P point mutation (*Ikzf1*^{L132P}) conserves overall protein expression, and has a B cell-specific phenotype with no effect on T cell development indicating that ZF1 is not required for T cells. Mice have reduced antibody responses to immunization and show a progressive loss of serum immunoglobulins compared to wildtype littermates. IKZF1^{L132P} overexpressed in NIH3T3 or HEK293T cells failed to localize to pericentromeric heterochromatin (PC-HC) and bind target DNA sequences. Co-expression of wildtype and mutant IKZF1 however, allows for localization to

Corresponding author: Anselm Enders; John Curtin School of Medical Research, 131 Garran Road, Acton ACT 2601, Australia; anselm.enders@anu.edu.au; (p) +61(0)261257605 (f) +61(0)61258512.

Authorship Contributions

Contribution: L.A.M., A.E., and C.C.G. identified the mouse strain. A.E., S.D.R., L.A.M., H.S.K., C.C.G., and B.B. designed the research. A.E., S.D.R., L.A.M., H.S.K., and B.B. analyzed results and wrote the paper; B.B., L.A.M., and H.S.K. made the figures; B.B., L.A.M., H.S.K., V.A., Y.S., Y.M., D.H., S.A.O., Z.Y., M.N., H.A.M., H.J.S., and I.A.C performed experiments and/or provided critical reagents and advice for this study. V.C. and T.D.A. analyzed RNAseq data.

[1]B.B. and L.A.M. contributed equally to this study

Conflict of Interest Disclosures

The authors declare no competing financial interests.

PC-HC and binding to DNA indicating a haploinsufficient mechanism of action for IKZF1^{L132P}. Furthermore, *Ikzf1*$^{+/L132P}$ mice have late onset defective immunoglobulin production, similar to what is observed in CVID patients. RNAseq revealed a total loss of *Hsf1* expression in follicular B cells suggesting a possible functional link for the humoral immune response defects observed in *Ikzf1*$^{L132P/L132P}$ mice.

Introduction

IKZF1, encoding for IKAROS, is a zinc finger transcription factor essential for immune cell development, homeostasis, and function (1). It was discovered to be of importance for both T and B cell development through the generation of an IKZF1 deficient mouse (*Ikzf1*$^{-/-}$). *Ikzf1*$^{-/-}$ mice have a complete block of lymphocyte development in the fetal liver, resulting in the absence of mature B and NK cells, yet surprisingly, some T cells develop postnatally (2) but show defects in TCR signaling in the thymus (3). Homozygous *Ikzf1*$^{-/-}$ mice are born at the expected frequency and survive into adulthood (2).

IKZF1 regulates transcriptional programs through the coordination of six zinc finger (ZF) domains; the first four are essential for regulating gene transcription through DNA binding, and the last two facilitate multimer formation as both a homodimer and as a heterodimer with IKZF1 and other family members (4). IKZF1 is able to regulate gene expression through both activation (4-6) and repression of gene transcription (6-10). In B cells, once lineage commitment has been established, IKZF1 regulates B cell-specific genes that are important for further development and B cell function (6, 11-16). Specifically, IKZF1 regulates the BCR-signaling cascade during pro- to pre-B cell development (6, 17, 18), thereby ensuring correct progression through the early phases of commitment to the B cell lineage and without which, B cells fail to develop. Additionally, germline *IKZF1* mutations in cohorts of common variable immunodeficiency (CVID) patients with low or absent B cells identified a crucial role for correct IKZF1 expression in maintaining normal B cell development and antibody production (19), as well as for self-tolerance of peripheral B cells (20) in humans.

The specific mechanism of action for IKZF1 however, is not fully understood. In mice, the second and third zinc finger domains (ZF2 and ZF3) bind to core GGGAA motifs (5) in both traditional DNA sequences, as well as in γ satellite regions in pericentromeric heterochromatin (PC-HC), thereby facilitating chromatin remodeling and changes in gene transcription (6, 7, 9, 21). In contrast, murine studies have shown that ZF1 and ZF4 are responsible for facilitating specificity by binding to flanking DNA sequences (22).

Our understanding of IKZF1 biology has been greatly enhanced through the analysis of many *Ikzf1* mouse models (summarized in Heizmann, et al. (23)). A dominant negative mutation removing ZF1, ZF2, and ZF3 in the IKZF1 DNA binding domain (*Ikzf1*$^{DN/DN}$) highlights how IKZF1 is important for hematopoietic stem cell commitment to the lymphoid lineage (24). *Ikzf1*$^{DN/DN}$ mice have a complete absence of all B and T cells and the majority die at a very young age due to increased opportunistic infections and septicemia (24). Mice heterozygous for this mutation (*Ikzf1*$^{+/DN}$) show no obvious B cell defects, yet lose the expression of wildtype IKZF1 in the thymus and spontaneously develop T cell-derived

leukemia and lymphoma (25). Recently, using CD23-CRE to conditionally delete IKZF1 in mature B cells, a conditional knock-out of IKZF1 was described (*Ikzf1*$^{B-}$) (26). *Ikzf1*$^{B-}$ mice develop splenomegaly and autoimmunity due to the attenuation of anergy induction in follicular B cells (FoB) cells (26). A single point mutation in ZF3 (H191R, *Ikzf1*$^{Plst/Plst}$) specifically disrupts the DNA binding ability of IKZF1 whilst still maintaining protein scaffold structure and expression (27). This mutation however, is embryonically lethal, but analysis of the fetal liver shows a complete loss of B and T cell development (27). Originally, it was postulated that the postnatal survival of *Ikzf1*$^{-/-}$ but not *Ikzf1*$^{Plst/Plst}$ mice, was because of a niche filling trait shared among Ikaros family members, that allows for compensation for the loss of total protein expression (27). In the case of a null mutation, Ikaros family members can step in and prevent total loss of function, but in the case of *Ikzf1*$^{Plst/Plst}$ mice, as IKZF1 protein expression has not been lost, there is no compensatory effects by other Ikaros family proteins. Interestingly, it was noted in Schjerven et al. (22) that *Ikzf1*$^{-/-}$ mice, originally bred from a mixed 129SV background, were attempted to be crossed to a pure C57/B6 background but failed likely due to embryonic lethality. This somewhat contradicts the idea that *Ikzf1*$^{-/-}$ can survive into adulthood due to compensation mechanisms employed by Ikaros family members when there is an absence of IKZF1 expression, but merely suggests that embryonic lethality is due to genetic differences across background strains.

Through these mouse models, it has become clear that IKZF1 is an essential transcription factor for both T and B cell development, yet the direct mechanism of how IKZF1 discerns between regulating either T or B cell transcriptional programs remains unknown. In attempts to address this question, multiple IKZF1 mouse models have isolated regulatory functions of IKZF1 that are exclusively important for either T or B lymphopoiesis. Removing *Ikzf1* exon 2 (*Ikzf1*$^{L/L}$), which is present in all IKZF1 isoforms, results in a B cell-specific block in development throughout multiple stages in the bone marrow (28). This mutation removes the amino acids expressed upstream of the N-terminal ZFs and results in the absence of expression of full-length IKZF1 but causes low level expression of a truncated form of IKZF1. Removing either ZF1 (*Ikzf1*$^{ZF1/ZF1}$) or ZF4 (*Ikzf1*$^{ZF4/ZF4}$) in mice demonstrated that these two ZFs are responsible for site-directed DNA binding and can selectively control T and B lymphopoiesis (22). Specifically, ZF1 seems to be responsible for controlling events leading to B cell development as *Ikzf1*$^{ZF1/ZF1}$ mice have a partial block of B cell development at the pro-B cell stage with very minimal T cell development defects (22). Conversely, *Ikzf1*$^{ZF4/ZF4}$ mice have a severe defect in T cell development in the thymus and a partial block of large pre-B cells in the bone marrow (22). This suggests that ZF4 is largely responsible for the development of T cells but is also required for normal B cell development, whilst ZF1 is dispensable for T cell development. Furthermore, *Ikzf1*$^{ZF4/ZF4}$ mice spontaneously develop thymic lymphomas, indicating a role for tumor suppression in ZF4. Because the authors were not able to identify a DNA motif specifically recognized by ZF1/ZF4 it is unclear whether the ZF1-specific role seen in *Ikzf1*$^{ZF1/ZF1}$ mice is solely caused by the loss of the respective ZF, or by the loss of the regulatory functions encoded by the upstream region of flanking sequences around ZF1 that are missing in these mice (22).

Whilst these mice demonstrate the plasticity of IKZF1 and clearly show that regulation of either B or T cell development can be associated with selective expression of ZF1 or ZF4,

these studies have generated *Ikzf1* mutations that also remove important regulatory regions of the protein. In the case of IKZF1, the removal of whole regulatory regions such as ZF1 or ZF4 can alter protein stability and result in reduced expression (22), potentially permitting compensation from other family members (27) and thereby obscuring any specific role of an individual zinc finger.

Through ENU-mutagenesis, we identified a mutant mouse with a novel point mutation in ZF1 located in the DNA binding domain of IKZF1. This L132P mutation does not abolish protein expression and still allows for dimerization, thus maintaining important structural integrity and avoids any need for niche-filling mechanisms from Ikaros family members. IKZF1^{L132P} mutant protein is unable to localize to PC-HC and bind target DNA sequences. This mutation therefore allows for the isolation of the role of IKZF1 ZF1 independently of any regulation by surrounding regions and compensation through other family members.

Materials and methods

The *Ikzf1*^{L132P} mice are available through the Australian phenome bank (https://pb.apf.edu.au).

DNA vectors are available upon request.

Mice

The *Ikzf1* L132P mutant strain was identified by flow cytometric screening of blood lymphocytes in third generation offspring of C57BL/6 mice treated with 3 × 90-100 mg/kg *N*-ethyl-*N*-nitrosourea (ENU). Variant calling from whole exome sequencing data was performed as previously described (29). All mice were generated and maintained on a C57BL/6NCrl background. For all mouse experiments, littermate controls were used. All mice were housed in specific pathogen–free conditions at the Australian National University Bioscience Research Services facility, and all animal procedures were approved by the Australian National University Animal Ethics and Experimentation Committee on protocols A2014/61, A2014/62 and A2017/54.

Flow cytometry

Analysis of peripheral blood was performed on 6-8 week old male and female mice as previously described (30). For analysis of lymphocyte development, 9-10 week old naïve male and female mice were sacrificed through CO_2 inhalation and organs collected in FACS buffer (1X PBS, 2.5% HI-BS, 0.1% NaN_3). Bone marrow was flushed out from the femur and tibia of one hind leg per mouse using a 26G needle. Single-cell suspensions for all organs were filtered through a 70μm cell strainer. Spleens were treated with red blood cell lysis buffer (8.99% w/v NH_4Cl, 1% w/v $KHCO_3$, 0.037% w/v EDTA, pH = 7.3) and then washed with FACS buffer. Cells were counted using a Beckman and Coulter Vi-CELL™ XR Cell Counter. $2x10^6$ cells were plated and stained for flow cytometry. Samples were acquired using a LSRFortessa™, or LSRFortessa™ X-20 (BD Bioscience) and analyzed using FlowJo software version 10.4.1 (FlowJo LLC).

For all samples, single cells (SSC-W vs SSC-H, FSC-W vs FSC-H) and live cells ($7AAD^-$) were selected for, followed by a lymphocyte gate (SSC-A and FSC-A). Cell subsets were gated as follows: total B cells ($B220^+$), pre-pro-B (bone marrow; $B220^+IgM^-IgD^-CD43^+CD24^-$), pro-B (bone marrow; $B220^+IgM^-IgD^-CD43^+CD24^{low}$), pre-B (bone marrow; $B220^+IgM^-IgD^-CD43^-CD24^{hi}$), immature B (bone marrow; $B220^+IgM^+IgD^-$, spleen; $B220^+CD93^+$), mature B (bone marrow; $B220^+IgM^+IgD^+$, spleen; $B220^+CD93^-$), follicular B (spleen; $B220^+CD93^-CD23^+CD21/35^{low}$), marginal zone B (spleen; $B220^+CD93^-CD23^-CD21/35^{hi}$), double negative (thymus; $CD19^-CD4^-CD8^-$), double positive (thymus; $CD19^-CD4^+CD8^+$), CD4 single positive (thymus; $CD19^-CD4^+CD8^-$, spleen; $CD3^+CD19^-CD4^+CD8^-$), CD8 single positive (thymus; $CD19^-CD4^-CD8^+$, spleen; $CD3^+CD19^-CD4^-CD8^+$), total T cells (spleen; $CD3^+$), germinal center B cells (spleen; $B220^+CD4^-Fas^+GL7^+$), T follicular helper cells (spleen; $TCR\beta^+CD19^-CD4^+CD8^-CXCR5^{hi}PD1^{hi}$) and memory B cells (spleen; $B220^+GL7^-Fas^-IgD^-CD38^{mid}CXCR5^{mid}$).

Total cell numbers were determined by calculating the percentage of each population as a fraction of live cells, and then multiplying this by the total viable cell count for each sample.

Immunoglobulin isotyping

Naïve male and female mice were bled at 6, 14, and 22 weeks of age. 200μl of blood was collected via retro-orbital bleed into tubes containing 10μl of 0.5M EDTA. Plasma was collected and stored at −20°C. Quantification of immunoglobulin isotypes were determined using the Mouse Isotyping Panel 1 kit from Meso Scale Discovery System and read using an MSD SECTOR instrument according to the manufacturer's instructions.

Immunizations and ELISA

Antibody responses to chicken gamma globulin (CGG) and *Bordetella pertussis* in 13-15 week old male and female mice were determined as described previously (31), except for the use of non-haptenated CGG. Antibody responses were determined 14 days post immunization. Long-lived memory responses to the recombinant circumsporozoite protein from *Plasmodium falciparum* (PfCSP) was analyzed in 15-23 week old mice as previously described (32), except only two immunizations of PfCSP in Alum were administered with two months between each dose. For analyzing germinal center dynamics, mice were immunized with $2x10^8$ sheep red blood cells i.v. and spleens collected 7, 10, or 15 days post immunization.

Plasmid preparation

Human IKAROS family zinc finger 1 (IKAROS) (*IKZF1*; NM_006060) vector information was previously described (19). Human IKAROS family zinc finger 3 (IKZF3/AIOLOS) ORF clone (pcDNA3.1-AIOLOS, NM_012481) and mouse *Ikzf1* ORF clone (pcDNA3.1(+)C-HA –*Ikzf1*, NM_001025597.2) were purchased from GenScript and *Ikzf1* was sub-cloned into pFlag-CMV2. Mutants for the IKZF1 were generated based on the site directed mutagenesis protocol using AccuPrime Pfx DNA Polymerase, followed by DpnI treatment (Life technologies).

Co-immunoprecipitation

HEK293T cells were co-transfected with pcDNA3-HA-Ikzf1 (WT or L132P mutant) and pFlagCMV2-Ikzf1 or pcDNA3.1+/C-DYK-IKZF3 (GenScript) using Effectene transfection reagent (Qiagen). Cell lysates were prepared 20h after transfection in lysis buffer (50mM Tris [pH 7.4], 150mM NaCl, 2mM EDTA, 0.5% Triton X-100, and halt protease and phosphatase inhibitor cocktail (Thermo fisher scientific). Total protein (500μg) was incubated with rabbit anti-FLAG polyclonal affinity antibody (Sigma). After 2h incubation at 4 °C on a rotating wheel, 50μl Protein A/G-agarose beads (Pierce) were added to each reaction and incubation was continued for another hour. Beads were washed three times with lysis buffer, samples were prepared and separated on a NuPAGE® Novex® 4-12% Bis-Tris Protein Gels (Life Technology). Subsequent western blot analysis was performed with the mouse anti-HA monoclonal antibody (Covance), and rabbit anti-FLAG polyclonal affinity antibody.

Immunofluorescence

NIH3T3 cells ($0.8\text{-}1\times10^5$) were seeded onto cover slips in 6 well plates. The next day, cells were transfected with the indicated plasmid using Effectene (Qiagen) according to the manufacturer's instructions. The cells were washed twice in PBS, fixed for 10 min in 4% paraformaldehyde and permeabilized for 15 min in 0.1% Triton X-100 in PBS at RT. The cells were then incubated for 30 min in blocking buffer (PBS with 10% FBS and 0.1% Triton X-100) then incubated for 2h with a mouse anti-HA monoclonal antibody (Covance), and/or a rabbit anti-Flag polyclonal affinity antibody (Sigma). The cells were washed with PBS and incubated for 1h with goat anti-mouse Alexa Fluor 488 (Life Technologies) and/or goat anti-rabbit Alexa Fluor 568 (Life Technologies) conjugated secondary antibodies in blocking buffer. Cells were washed again and stained with DAPI for 5 minutes before a final wash and were then mounted on slides using VECTASHIELD Mounting Medium (Vector Laboratories). Images were collected using ZOE fluorescent cell imager (Bio-Rad) original magnification 175x. Red and green channels were cropped and merged after acquisition using ImageJ software.

Lightshift chemiluminescent EMSA

HEK293T cells were transfected with pCMV6-AC-Myc-DDK-IKZF1 or pFlag CMV2-Ikzf1 WT or mutant and nuclear extracts were prepared using NE-PER nuclear extract kit according to the manufacturer's instruction (Thermo Fisher Scientific). Gel mobility shift assays were performed using Lightshift Chemiluminiscent EMSA kit (Thermo Fisher Scientific) according to the manufacturer's instruction. DNA-protein complexes were separated on 6% Novex TBE gels with 0.5x TBE. γ-satellite from human chromosome 8 (γ-Sat8) (Forward: 5'-BIOTIN-GCGAGACCGCAGGGAATGCTGGGAGCCTCCC, Reverse: 5'-BIOTIN- GGGAGGCTCCCAGCATTCCCTGCGGTCTCGC)(33); IKAROS consensus-binding sequence 1 (IK-bs1) (Forward: 5'-BIOTIN- TCAGCTTTTGGGAATACCCTGTCA, Reverse: 5'-BIOTIN-TGACAGGGTATTCCCAAAAGCTGA).(5, 33)

Bulk RNA sequencing and analysis

Live FoB cells ($B220^{+}CD93^{-}CD23^{+}CD21/35^{low}$) from the spleens of three *Ikzf1*$^{+/+}$ and three *Ikzf1*$^{L132P/L132}$ female mice were FACS sorted and lysed in 1mL of TRIzol (Thermo Fisher Scientific) and stored at −80°C. Cells were thawed and incubated with 200μl chloroform. The aqueous phase was removed and a second round of chloroform extraction performed before precipitating with equal volumes of isopropanol. RNA was then washed twice with 70% ethanol and final RNA solution analyzed for quantity and quality on an Agilent Technologies 2100 Bioanalyzer with all samples scoring a RIN of >8. RNAseq libraries were prepared using Illumina® TruSeq® Stranded mRNA Library Prep Kit according to the manufacturer's instructions and samples sequenced with mid output 150 cycles flowcells with 75bp paired end reads on the Illumina NextSeq 500.

Estimation of transcript-level abundance was obtained by running Salmon with the default parameters (34) and the reference index created from GRCm38's transcriptome sequence, Ensembl release 97 (35). The abundance data was imported into R (36) using tximport (37) and pre-filtered so that the minimum total read count across all samples is at least 10. The differential expression analysis was performed by DESeq2 (38) where the adjusted p-value cutoff at FDR level of 0.1 was applied.

The RNA-seq data has been submitted to Array Express under accession number E-MTAB-9975 (https://www.ebi.ac.uk/arrayexpress/experiments/E-MTAB-9975).

Statistical analyses

Data was analyzed using R version 3.3.1. Data was fit to a linear model using lmerTest (39). For flow cytometry total cell number data, each individual cell population mean was analyzed against the genotype. Where possible, repeat experiments were used as blocking factors to account for any variability between experiments. A one-way ANOVA was then used to determine any interaction between genotype and cell population mean. Pairwise comparisons were determined using emmeans, comparing all genotypes within a cell population. The same approach was used for antigen-immunization ELISAs except the response to individual antigens was compared with the genotype.

For naïve immunoglobulin isotype quantification, data was gathered and fit to a linear model as above. Any interaction between genotype, age, and isotype was determined by performing a one-way ANOVA. As plasma samples were collected at different times, any variation between blood collection and length of storage of plasma was accounted for by including blood collection batches as a blocking factor. Output indicated any differences in trends observed within a genotype across all 3 time points and reported any differences between genotypes. As only IgG1 was found to be significantly different from the other isotypes analyzed, a one-way ANOVA and pairwise comparison using "emmeans" of just this sample set was performed, comparing the mean of each genotype across each time point, again using blood collection batch as a blocking factor. Not significant (n.s.) $p>.05$, *$p\leq.05$, **$p\leq.01$, *** $p\leq.001$, **** $p\leq.0001$.

Results

Discovery of mutation

In an *N*-ethyl-*N*-nitrosourea (ENU) mutagenesis screen to identify genes involved in lymphocyte development we identified several related mice with low frequencies of mature B cells in their blood. Analysis of exome sequencing data of founder G1 mice revealed a T to C substitution of nucleotide 11:11748545 (GRCm38/mm10). This converts leucine (cTc) at position 132 within IKZF1 ZF1 to proline (cCc) (Supplemental Figure 1 A, B).

Effect on lymphopoiesis

To analyze the impact of the $Ikzf1^{L132P}$ mutation on lymphocyte development; bone marrow, spleen, and thymus of 9-10 week old naïve mice were analyzed by flow cytometry (Figure 1). Similar to results reported from $Ikzf1^{ZF1/ZF1}$ mice (22) as well as CVID patients with missense mutations in ZF2 and ZF3 of *IKZF1* (19, 20), mice homozygous for the L132P mutation ($Ikzf1^{L132P/L132P}$) showed a partial block of B lymphopoiesis at the transition from pro- to pre-B cells and a subsequent reduction of all proceeding development stages in the bone marrow (Figure 1 A). This caused a reduction in the number of B cells in the spleen and peripheral blood (Figure 1 B, C). Within the spleen, the number of immature and mature follicular B cells were significantly reduced in homozygotes (Figure 1B). Marginal zone B cells however were unaffected and maintained at normal numbers (Figure 1B).

Heterozygous mice ($Ikzf1^{+/L132P}$) showed normal B cell development in the bone marrow (Figure 1A) and had normal numbers of immature B cells in the spleen (Figure 1B). The number of follicular B cells however, were significantly reduced but still increased compared to homozygotes (Figure 1B). Similarly, the frequency of B cells in the blood of $Ikzf1^{+/L132P}$ mice are slightly but significantly decreased compared to wildtype littermates (Figure 1C).

Remarkably, the L132P mutation did not affect T cell development with normal numbers of major thymic populations present in both heterozygotes and homozygotes (Figure 1D). Similarly, there were no differences in splenic T cell numbers in heterozygotes and homozygotes compared to wildtype littermates (Figure 1E). This confirms a differential role for each ZF in lymphocyte development and suggests that IKZF1 ZF1 is essential for murine B cell, but not T cell development (22, 28).

Effect on the humoral immune response

Mutations within the DNA binding domain of *IKZF1* in CVID patients result in the inability to maintain normal amounts of serum immunoglobulins over time (19, 20). To determine whether a similar effect on secreted immunoglobulin production can be seen in $Ikzf1^{L132P}$ mice, plasma was collected from naïve mice at 6, 14, and 22 weeks of age and total IgM, IgG1, IgG2a, IgG2b, and IgA concentrations measured (Figure 2A). While no statistically significant differences were detected for most isotypes, IgG1 was significantly reduced in older heterozygous and homozygous mice.

Next, we wanted to determine whether *Ikzf1*^{L132P} mice were able to elicit proper humoral immune responses following immunization with formalin-fixed *Bordetella pertussis*, and chicken-gamma-globulin (CGG) in Alum. Levels of antigen-specific antibodies from the plasma of immunized mice were determined via ELISA (Figure 2B). *B. pertussis* predominantly induces isotype switching to IgG2a[b], whilst CGG in Alum mainly induces switching to IgG1. Both heterozygotes and homozygotes produced significantly fewer *B. pertussis*-specific IgG2a[b] than wildtype littermates, yet demonstrated a normal IgG1 antibody response to CGG (Figure 2B). We therefore questioned whether this was the result of a specific antigen-defect or a defect in isotype switching. We then tested for CGG-specific IgG2a[b] and found reduced concentrations in both heterozygous and homozygous mice suggesting L132P is important for IgG2a[b] isotype switching after immune challenge. These results combined with a reduction in total IgG1 concentrations in ageing mice indicates a defect in the elicitation of a humoral immune response in both *Ikzf1*$^{+/L132P}$ and *Ikzf1*$^{L132P/L132P}$ mice.

High-affinity antigen-specific antibodies are derived from the germinal center (GC) within secondary lymphoid organs after antigen stimulation and B cell activation. To assess whether the differentiation into GC B cells was normal in *Ikzf1*^{L132P} mice, mice were immunized with sheep red blood cells (SRBCs) and the frequency of GC B cells in the spleen was determined via flow cytometry 7, 10, and 15 days after immunization (Figure 2C and Supplemental Figure 2). Consistent with *Ikzf1*$^{B-}$ mice (26), both *Ikzf1*$^{+/L132P}$ and *Ikzf1*$^{L132P/L132P}$ mice had reduced frequencies of GC B cells compared to wildtype mice across all timepoints. Furthermore, frequencies of T follicular helper (Tfh) cells were significantly reduced in heterozygotes and were even further significantly reduced in homozygotes (Supplemental Figure 2). Total numbers of memory B cells were also significantly reduced in the spleen of both heterozygotes and homozygotes 15 days post SRBC immunization (Figure 2D), suggesting the initial memory B cell output is reduced in mutant mice. Lastly, to test the long-lived memory response, we immunized mice with recombinant *Plasmodium falciparum* circumsporozoite protein (PfCSP); a model antigen for inducing a T-dependent B cell memory response (32). Using a prime-boost strategy with a two-month interval between primary and secondary immunizations, this showed a significant decrease in PfCSP-specific IgG in the serum of homozygous mice 5 days post boost (Figure 2E). Taken together, these results indicate a profound and long-lasting defect in the germinal center and humoral immune responses in *Ikzf1*^{L132P} mice.

Protein-protein interactions and DNA binding

IKZF1 functions through the formation of homodimers or heterodimers with other Ikaros family members, such as IKZF3 (Aiolos) (40). This process is facilitated through interactions of the dimerization domain that includes ZF5 and ZF6. The L132P mutation occurs in ZF1 in the IKZF1 DNA binding domain leaving the dimerization domain intact, leading to the hypothesis that the dimerization capability of IKZF1^{L132P} would remain unaffected. Protein-protein interactions were tested through co-immunoprecipitations (Co-IPs) and the successful formation of IKZF1 homodimers and heterodimers were confirmed by western blot (Figure 3A). Murine DNA sequences of wildtype and L132P mutant *Ikfz1* isoform 1 (Ik1) were cloned into Flag- and/or HA- tagged vectors and subsequently co-

transfected and overexpressed in HEK293T cells. A Co-IP was performed with an anti-Flag antibody and a western blot was then performed on the pull-down product and probed for Flag and HA. Positive staining for HA indicated that the L132P mutation allows for the formation of homodimers (Figure 3A left panels). To test heterodimer formation, wildtype and mutant IKZF1 were co-expressed with IKZF3 and a Co-IP performed as above. Similarly to IKZF1-IKZF1 interactions, IKZF1^{L132P} was able to successfully form heterodimers with IKZF3 (Figure 3A right panels). The L132P ZF1 mutation therefore does not affect IKZF1 homodimerization or heterodimerization with IKZF3 and any defects observed are not due to the absence of IKZF1 polymers.

As the dimerization abilities of IKZF1 have not been altered in L132P mutants, we next wanted to see if DNA binding was affected. Transcriptional repression by IKZF1 requires the localization of IKZF1 and target genes to PC-HC (7, 10). To visualize this, NIH3T3 fibroblast cells were transfected with either wildtype or L132P mutant *Ikzf1*, and protein localization was visualized through fluorescence microscopy (Figure 3B). Wildtype IKZF1 shows punctate staining within the nucleus, indicating localization to PC-HC. When transfected with *Ikzf1*^{L132P} however, a diffuse staining pattern with no punctate foci can be observed, thus demonstrating that IKZF1^{L132P} is unable to localize to PC-HC. To test the ability of a wildtype-mutant IKZF1 dimer to bind PC-HC, NIH3T3 cells were co-transfected with 1:1 ratio of wildtype and L132P mutant *Ikzf1*, and PC-HC localization was visualized (Figure 3B). Punctate staining of both wildtype and mutant IKZF1 indicates that wildtype IKZF1 has the ability to bring the mutant protein to PC-HC and that the mutant protein does not interfere with the chromatin localization function of the wildtype protein. The IKZF1^{L132P} mutation therefore is not a dominant negative mutation.

To test the interaction between IKZF1^{L132P} with IKZF3 with regards to PC-HC localization, NIH3T3 cells were co-transfected with 1:1 ratio of wildtype *IKZF3* and either wildtype *Ikzf1* or L132P mutant *Ikzf1*. PC-HC localization of both IKZF3 and IKZF1 was then visualized (Figure 3B). While WT IKZF1/IKZF3 heterodimers localized to PC-HC, heterodimers between IKZF3 and IKZF1^{L132P} showed a diffuse staining pattern with no discernible foci, similar to IKZF1^{L132P} alone. Interestingly, this suggests that the L132P mutation has a dominant negative effect on wildtype IKZF3, but not wildtype IKZF1.

To determine if DNA binding is directly affected by the L132P mutation, an electrophoretic mobility shift assay (EMSA) was performed with IK-bs1, a known IKZF1 consensus sequences. HEK293T cells were transfected with either empty vector, Flag-tagged wildtype or L132P mutant *Ikzf1*, or were co-transfected with 1:1 ratio of wildtype and L132P mutant *Ikzf1*. Nuclear fractions were incubated with biotinylated IK-bs1 and DNA binding was determined by probing for biotin expression after electrophoretic separation (Figure 3C). A western blot for FLAG expression was performed on total protein lysate as a loading control (Figure 3C, bottom panel). IKZF1 dimer and multimer formation with IK-bs1 can be observed in wildtype conditions. Likewise, when wildtype and mutant IKZF1 are present, DNA binding can be observed further confirming that when in heterozygosity, IKZF1^{L132P} is not interfering with wildtype IKZF1. As expected, when only L132P mutant IKZF1 is present, DNA binding is lost with no detectable bands, similar to the empty vector negative control. Furthermore, we used a luciferase reporter assay in HEK293 cells to test the ability

of IKZF1^{L132P} to repress the activity of target genes (Supplemental Figure 3A) based on Ikaros family binding sites reported in Morgan et al. (1997) (40) and Kelley et al. (1998) (41). As expected, IKZF1^{L132P} was unable to repress the known target, IK-bs4 (7), similar to the empty vector control, whilst wildtype IKZF1 showed significant downregulation of luciferase activity.

To test for any functional molecular differences between murine and human IKZF1, we also performed all assays using human IKZF1 wildtype and L132P mutant transcripts (Supplemental Figure 3B, C & Supplemental Figure 4). Additionally, we also tested for human IKZF1^{L132P} binding to γ-Sat8, another known target for IKZF1 binding and found that similarly to IK-bs1, IKZF1^{L132P} was unable to bind to γ-Sat8. Amino acid L132 is conserved between human and mouse (1) (Ik1 isoform) and results from Co-IP, PC-HC localization, and EMSAs are consistent between human and mouse vectors, therefore confirming at the molecular level at least, murine IKZF1^{L132P} acts no differently from human IKZF1^{L132P}.

Absence of HSF1 expression underpins defects in humoral immune response

IKZF1 is a zinc finger transcription factor that is able to both activate (4-6) and repress gene transcription (6-10). To gain an understanding of how the IKZF1^{L132P} mutation is affecting global gene expression, we performed RNAseq on wildtype and L132P mutant follicular B (FoB) cells. As FoB cells are the primary B cells that respond to foreign antigen stimulation in secondary lymph node organs, RNAseq of these cells allows for potential insight into the differences in the B cell transcriptional program that could be underpinning the humoral immune response defect in *Ikzf1*^{L132P} mice. We first looked at genes with greater than 2-fold difference in expression compared to wildtype and found 190 differentially regulated genes (Figure 4A & Supplemental Table 1). Of these, 30 were downregulated in *Ikzf1*$^{L132P/L132P}$ FoB cells and 160 were upregulated. Notably, *Hsf1* expression was completely absent in homozygous FoB cells (Figure 4B). *Hsf1* encodes for heat shock factor 1 and is a transcriptional regulator that governs the heat-related stress response (42). It has been shown to be differentially expressed in *Ikzf1*^{N159A} pre-B cells but is not a direct target of IKZF1 in pre-B cells (14) or FoB cells (26). HSF1 has important roles in mammalian development (42) and the immune system (43-45). Importantly, mice deficient in HSF1 (*Hsf1*$^{-/-}$) have a B cell intrinsic reduction in total numbers of GC B cells after SRBC immunization and reduced titers of antigen-specific IgG2a after NP-CGG immunization (45). *Hsf1*$^{-/-}$ mice essentially exactly recapitulate the humoral immune defect we see in the *Ikzf1*^{L132P} mice and therefore could explain the reduced capacity for B cell function in *Ikzf1*$^{+/L132P}$ and *Ikzf1*$^{L132P/L132P}$ mice. Finally, we compared the 190 differentially regulated genes in *Ikzf1*$^{L132P/L132P}$ FoB cells with 113 genes differentially regulated in FoB cells from IKZF1 B cell-specific knock-out mice (*Ikzf1*$^{B-}$) (26) (Figure 4C). Surprisingly, we only found 9 genes common to both data sets (Figure 4D), thus indicating very different regulatory profiles of B cells that are completely deficient in IKZF1 compared with a specific point mutation. *Hsf1* was not found to be differentially expressed in *Ikzf1*$^{B-}$ FoB cells. The lack of similarity between the two data sets provides further evidence of the novelty of the *Ikzf1*^{L132P} mutation and demonstrates unequivocally that the L132P mutation does not induce a null allele in *Ikzf1*.

Discussion

The importance of IKZF1 in lymphoid development and function has been widely documented. The majority of studies however, have involved mutations in IKZF1 that abolish both protein function and stability. The absence of correct maintenance of IKZF1 expression allows for compensation through other family members (27) and does not allow for the understanding of the exact role of IKZF1 in lymphoid development independent of its family members. By altering the ability of IKZF1 to bind target DNA through an amino acid substitution in ZF1, yet still maintaining protein expression, we were able to elucidate the specific role of IKZF1 in the development and function of the murine immune system. Our ENU-induced L132P mutation demonstrates that ZF1 is responsible for B cell development yet is dispensable for regulating T cell development in mice. This clarifies previous work by Schjerven et al. (22) who showed that a complete loss of ZF1 expression specifically affected B cells and not T cells. In that study however, it is not clear whether the effect was specific to ZF1, or caused by the loss of upstream regions that have been suggested to have some regulatory effects (22). Similarly, deletion of exon 2, which lies upstream of the DNA binding domain and is present in all isoforms, results in a B cell-specific defect (28). As this mutation also removes some regulatory regions before the proceeding ZF domains, it does not conclusively implicate ZF1 as being exclusive to B cell development. Work by Papathanasiou et al. (27) demonstrated that IKZF1 works in a tight balance with other Ikaros family members and that loss of IKZF1 results in a niche-filling effect by other Ikaros family proteins. B cell-specific mutations described by Schjerven et al. (22) and Kirstetter et al. (28) result in loss of expression and/or stability of full-length IKZF1. This suggests that the B cell-specific phenotypes observed in the *Ikzf1*$^{ZF1/ZF1}$ and *Ikzf1*$^{L/L}$ mice could be due to an altered ratio of predominant Ikaros family members, rather than the specific loss of ZF1 function by itself. The IKZF1^{L132P} mutation however, preserves expression of full- length IKZF1 (Figure 3C) and maintains dimerization capabilities both as a homodimer and heterodimer. Any effect on B cell development can therefore be attributed to loss of DNA binding specificity that is solely attributed to a loss of ZF1 function.

Interestingly, the murine L132P mutation only induces a partial block of B cell development in homozygote mice at the pro-B cell stage (Figure 1A), contrasting with more severe findings in other IKZF1 mouse models (2, 6, 17, 18, 24, 27). A possible explanation could be that IKZF1 binding to select DNA sequences is not completely abolished in *Ikzf1*$^{L132P/L132P}$ mice. The detection of transcripts that are known to be directly regulated by IKZF1 in FoB cells in *Ikzf1*$^{L132P/L132P}$ mice (Figure 4 & Supplemental Table 1) shows that IKZF1^{L132P} is still able to activate and repress some target genes. Whilst we have checked binding to IK-bs1 and γ-Sat8 and shown that IKZF1^{L132P} cannot bind directly to these sequences (Figure 3C & Supplemental Figure 3), both of these genes are located within heterochromatin and our results do not rule out the possibility of IKZF1^{L132P} binding to site-specific DNA promoter sequences that are not located within PC-HC.

It is interesting to note that *Ikzf1*$^{+/L132P}$ mice showed no defects in B cell development, yet have reduced numbers of follicular and mature B cells in the spleen and reduced frequency of circulating B cells in the peripheral blood, as well as normal numbers of marginal zone B

cells (Figure 1C). The normal numbers of marginal zone B cells in both *Ikzf1*$^{+/L132P}$ and *Ikf1*$^{L132P/L132P}$ mice indicates that IKZF1 might not be essential for the maintenance of certain resident B cell niches. Yet the decreased numbers of mature B cells in the periphery in *Ikzf1*$^{+/L132P}$ mice suggests that correct IKZF1 expression is required for either survival or maintenance of B cells within secondary lymphoid organs and the circulating lymphocyte pool.

To determine the functional capacity of IKZF1^{L132P} mutant B cells, we analyzed the primary and secondary B cell response to immunization with specific and non-specific antigens (Figure 2). The absence of germinal centers as well as significantly reduced memory B cell output in both *Ikzf1*$^{+/L132P}$ and *Ikzf1*$^{L132P/L132P}$ after SRBC immunization (Figure 2C & D) is further evidence that IKZF1 is required not only for B cell development, but also B cell function. As Tfh cells are known to be dependent on the number of GC B cells and general GC formation (46), it is unsurprising that Tfh frequencies were also reduced in *Ikzf1*^{L132P} mice (Supplemental Figure 2). As *Ikzf1*$^{B-}$ mice also fail to induce normal numbers of GC B cells (26), this argues that the loss of GC B cells is a B cell intrinsic defect causing a secondary Tfh cell effect.

To tease out the effects of L132P on the function of IKZF1, we performed a series of molecular analyses testing the ability of IKZF1^{L132P} to dimerize, localize to PC-HC, and directly bind to target DNA sequences (Figure 3). This showed that PC-HC localization and DNA binding were abolished in IKZF1^{L132P} only conditions, yet dimerization was maintained. When wildtype IKZF1 was co-expressed however, IKZF1^{L132P} was able to be recruited to PC-HC and allow for subsequent DNA binding, showing that the L132P mutation does not act in a dominant negative manner, but rather that IZKF1^{L132P} is acting in a haploinsufficient manner in *Ikzf1*$^{+/L132P}$ mice, causing some loss of B cells and antibody deficiency. This corresponds with known *IKZF1* haploinsufficient mutations (19) and contrasts with known *IKZF1* dominant negative mutations (47).

It is surprising that when mutant IKZF1 is co-expressed with IKZF3, PC-HC localization is lost (Figure 3B). As the L132P mutation does not affect dimerization between IKZF1 and IKZF3, this defect must be driven by the lack of recruitment of heterodimer protein complexes to PC-HC, rather than the inability for protein complexes to form in the first place. Similar results have been observed in IKZF1 Ik-6 (40), which lacks the entire DNA binding domain but maintains the dimerization domain (4), as well as in CVID patients with an *IKZF1*$^{+/N159S}$ dominant-negative mutation (47). This shows that the localization of PC-HC and foci formation of IKZF1/IKZF3 heterodimers is primarily dependent on IKZF1. It is possible that in the context of IKZF1/3 heterodimers, IKZF1 is essential for localizing to PC-HC whilst IKZF3 is essential for recruitment of target genes to PC-HC in order to silence transcription. It remains to be seen in future studies if IKZF1^{L132P}/IKZF3 heterodimers are able to regulate gene transcription outside of PC-HC. Given the many functions of IKZF1 on regulating gene transcription, including through the extensive opening and closing of chromatin and the formation of enhancers (48), comprehensive further studies will be required to fully understand the molecular mechanism causing the reduced B cell survival in homozygous *Ikzf1*$^{L132P/L132P}$ mice. These studies will require

analysis of both chromatin status, expression of Line1, IAP and other repetitive elements that could cause a toxic effect on cells when overexpressed.

It is tempting to speculate that the failure to localize to PC-HC observed for IKZF1/3 heterodimers containing IKZF1 variants found in both humans and mice with B cell defects underlies the block in B cell development, but confirmation of this will require further experiments beyond the scope of the present study. It is unlikely however, that the absence of IKZF1/3 dimers results in attenuation of B cell development in pro-B cells in *Ikzf1*$^{L132P/L132P}$ mice as IKZF3 is generally upregulated in pre-B cells, rather than pro-B cells (49). Furthermore, IKZF3 deficient mice (*Ikzf3*$^{-/-}$) exhibit a very different phenotype from what is described here, with an increase in concentrations of serum IgG and IgE in naiïve mice and the absence of marginal zone B cells as well as development of autoimmunity and B cell lymphomas (50). Without the availability of a B cell conditional IKZF3 knockout it is difficult to tease out which of these phenotypes is B cell intrinsic. Regardless, the obvious differences between *Ikzf3*$^{-/-}$ and *Ikzf1*$^{L132P/L132P}$ mice suggests that the absence of functional IKZF1/3 dimers in *Ikzf1*$^{L132P/L132P}$ mice does not entirely underpin the L132P mutant phenotype.

Interestingly, RNAseq identified a complete absence of *Hsf1* expression in *Ikzf1*$^{L132P/L132P}$ FoB cells (Figure 4A & B) demonstrating that IKZF1 L132 is crucial for *Hsf1* either indirectly or directly. This confirms previous work demonstrating that removing the ability for IKZF1 to bind to DNA results in the downregulation of *Hsf1* (14), despite it not being a direct target of IKZF1 (14, 26). This suggests that one or more unknown intermediary protein(s) must be acting upon the expression of *Hsf1* in the context of IZKF1 being unable to bind DNA. Absence of HSF1 in mice leads to a loss of *Bcl6* upregulation and subsequent reduction in GCB and Tfh cell numbers in a B cell intrinsic manner (45). Furthermore, *Hsf1*$^{-/-}$ mice have reduced basal and antigen-specific IgG2a production (44, 45). As *Ikzf1*^{L132P} mutant mice can produce antigen-specific IgG1 but not IgG2a (Figure 2B), this suggests that the absence of HSF1 leads to aberrant IgG2a switching.

Recently, conditional deletion of IKZF1 in B cells (*Ikzf1*$^{B-}$) has led to the discovery of the role of IKZF1 in anergy induction (26). When we compared genes that are differentially expressed in *Ikzf1*$^{B-}$ and *Ikzf1*$^{L132P/L132P}$ FoB cells, only 9 genes were found to be significant in both data sets (Figure 4 C&D) with 4 of these genes being directly bound by IKZF1 (26). This demonstrates that the L132P mutation does not cause a functional knock-out of IKZF1 and is therefore a novel mutation in regards to IKZF1-dependent B cell function. It should be noted however, that the controls used to determine differential gene expression in *Ikzf1*$^{B-}$ mice were in fact heterozygous for IKZF1-deletion (*Ikzf1*$^{B+}$) (26). Whilst no difference is noted for B cell development in *Ikzf1*$^{B+}$ mice compared to wildtype, *Ikzf1*$^{+/L132P}$ mice also have normal B cell development but significantly reduced B cell function compared to wildtype. It is therefore possible that differences in gene expression between *Ikzf1*$^{B-}$ and *Ikf1*$^{L132P/L132P}$ could be due to a lack of similar controls.

The *Ikzf1*^{L132P} mutation provides insight into the complicated role of IKZF1 in B cell development and function but the importance of these mice also extends to human disease as heterozygous *Ikzf1*$^{+/L132P}$ mice depict three of the main features of CVID: late onset, basal

IgG1 production defects, and reduced humoral immunity. When in heterozygosity, the L132P murine mutation causes no defects in B cell development yet causes a functional defect in the B cell response. Mice show progressive reduction of basal levels of serum IgG1 compared with wildtype littermates and have a limited humoral response to antigen stimulation. The molecular effects of this mutation mimic multiple studies modeled on known pathogenic *IKZF1* mutations in CVID cohorts (19, 47). Furthermore, the reduced B cell response is not apparent early in life but appears during adulthood, mimicking a key feature seen in CVID patients. The crucial role of IKZF1 for the normal functioning of the immune system is highlighted by the presence of genomic and somatic mutations throughout all parts of the gene, with particular clusters located in the 6 ZFs in patients presenting with primary immunodeficiencies (PIDs) or acute lymphoblastic leukemia (51). So far, 22 different mutations have been described in patients with immunodeficiencies. The majority of the mutations are located in ZF2 but other mutations have been found in the N-terminus before ZF1, in ZF3, ZF4, and ZF6. Currently, no variants in ZF1 and ZF5 have been found in PID patients. Interestingly, with the increasing number of patients identified, a phenotype-genotype correlation is now emerging (52), but further studies on more patients and ideally on matching mouse models will be required to fully understand the effect of specific mutations.

Altogether, the findings in the $Ikzf1^{+/L132P}$ mice recapitulate the main immunophenotypic features seen in CVID patients, independent of their underlying genetic defect, therefore suggesting that the $Ikzf1^{+/L132P}$ mouse could provide a representative model for human CVID disease.

The $Ikzf1^{L132P}$ mutant mice add to the understanding of IKZF1 biology and provide a potential avenue for further investigation into CVID diseases in humans. Furthermore, they provide additional evidence for the B cell-specific role of IKZF1 ZF1, independent of essential activities encoded by the surrounding region. Whilst ZFI has previously been shown to be critical for B cell development and nonessential for T cell development (22), we show here that the loss of ZF1 binding but maintenance of correct familial dimerization abilities is responsible for the failure to complete development in a significant proportion of B cells with no effect on T cell development. Functional studies demonstrated that this defect also extends to antibody production, providing evidence for the role of IKZF1 specifically in the humoral immune response. Additionally, failure to upregulate *Hsf1* was identified as a possible cause of defunct germinal centers and antibody production. Lastly, the $Ikzf1^{+/L132P}$ mice mimic CVID in humans and can provide a suitable model for which to study CVID onset and potential therapies.

Supplementary Material

Refer to Web version on PubMed Central for supplementary material.

Acknowledgments

This study used National Collaborative Research Infrastructure Strategy -enabled Australian Phenomics Network and Bioplatforms Australia infrastructure and we thank the Australian Phenomics Facility Next Generation Sequencing team and the Biomolecular Resource Facility at the John Curtin School of Medical Research for

performing whole exome and RNA sequencing. We thank the Genome Informatics group for exome sequencing analysis and the staff at the Australian Phenomics Facility for animal husbandry. We also thank the National Computational Infrastructure (Australia) for continued access to significant computation resources and technical expertise.

[2] This work was funded by National Institutes of Health grant U19-Al100627 and by the National Collaborative Research Infrastructure Strategy. This work was also supported by the Intramural Research Program, National Institutes of Health Clinical Center. The content of this article does not necessarily reflect the views or policies of the Department of Health and Human Services, nor does mention of trade names, commercial products, or organizations imply endorsement by the US government. B.B. supported by an Australian Government Research Training Program (RTP) Scholarship, and the Adam J. Berry Memorial Fund. A.E. was supported by Australian National Health and Medical Research Council (NHMRC) Career Development Fellowship 1035858 and NHMRC Grant 1079648. C.C.G. was supported by NHMRC Fellowships 585490 and 1081858.

Abbreviations used in this article:

[3]

CGG	chicken gamma globulin
Co-IP	co-immunoprecipitation
CVID	combined variable immunodeficiency
ENU	*N*-ethyl-*N*-nitrosourea
FoB	follicular B cell
PC-HC	pericentromeric heterochromatin
PfCSP	*Plasmodium falciparum* circumsporozoite protein
PID	primary immunodeficiency
ZF	zinc finger

References

1. Molnár Á, Wu P, Largespada DA, Vortkamp A, Scherer S, Copeland NG, Jenkins NA, Bruns G, and Georgopoulos K. 1996. The Ikaros gene encodes a family of lymphocyte-restricted zinc finger DNA binding proteins, highly conserved in human and mouse. The journal of Immunology 156: 585–592. [PubMed: 8543809]
2. Wang J-H, Nichogiannopoulou A, Wu L, Sun L, Sharpe AH, Bigby M, and Georgopoulos K. 1996. Selective defects in the development of the fetal and adult lymphoid system in mice with an Ikaros null mutation. Immunity 5: 537–550. [PubMed: 8986714]
3. Winandy S, Wu L, Wang J-H, and Georgopoulos K. 1999. Pre–T cell receptor (TCR) and TCR-controlled checkpoints in T cell differentiation are set by Ikaros. Journal of Experimental Medicine 190: 1039–1048.
4. Sun L, Liu A, and Georgopoulos K. 1996. Zinc finger-mediated protein interactions modulate Ikaros activity, a molecular control of lymphocyte development. The EMBO Journal 15: 5358. [PubMed: 8895580]
5. Molnar A, and Georgopoulos K. 1994. The Ikaros gene encodes a family of functionally diverse zinc finger DNA-binding proteins. Molecular and cellular biology 14: 8292–8303. [PubMed: 7969165]
6. Schwickert TA, Tagoh H, Gültekin S, Dakic A, Axelsson E, Minnich M, Ebert A, Werner B, Roth M, and Cimmino L. 2014. Stage-specific control of early B cell development by the transcription factor Ikaros. Nature immunology 15: 283. [PubMed: 24509509]

7. Cobb BS, Morales-Alcelay S, Kleiger G, Brown KE, Fisher AG, and Smale ST. 2000. Targeting of Ikaros to pericentromeric heterochromatin by direct DNA binding. Genes & development 14: 2146–2160. [PubMed: 10970879]
8. Kim J, Sif S, Jones B, Jackson A, Koipally J, Heller E, Winandy S, Viel A, Sawyer A, and Ikeda T. 1999. Ikaros DNA-binding proteins direct formation of chromatin remodeling complexes in lymphocytes. Immunity 10: 345–355. [PubMed: 10204490]
9. Trinh LA, Ferrini R, Cobb BS, Weinmann AS, Hahm K, Ernst P, Garraway IP, Merkenschlager M, and Smale ST. 2001. Down-regulation of TDT transcription in CD4+ CD8+ thymocytes by Ikaros proteins in direct competition with an Ets activator. Genes & development 15: 1817–1832. [PubMed: 11459831]
10. Brown KE, Guest SS, Smale ST, Hahm K, Merkenschlager M, and Fisher AG. 1997. Association of transcriptionally silent genes with Ikaros complexes at centromeric heterochromatin. Cell 91: 845–854. [PubMed: 9413993]
11. Nera KP, Alinikula J, Terho P, Narvi E, Törnquist K, Kurosaki T, Buerstedde JM, and Lassila O. 2006. Ikaros has a crucial role in regulation of B cell receptor signaling. European journal of immunology 36: 516–525. [PubMed: 16482514]
12. Reynaud D, Demarco IA, Reddy KL, Schjerven H, Bertolino E, Chen Z, Smale ST, Winandy S, and Singh H. 2008. Regulation of B cell fate commitment and immunoglobulin heavy-chain gene rearrangements by Ikaros. Nature immunology 9: 927–936. [PubMed: 18568028]
13. Heizmann B, Kastner P, and Chan S. 2013. Ikaros is absolutely required for pre-B cell differentiation by attenuating IL-7 signals. Journal of Experimental Medicine 210: 2823–2832.
14. Vidal IF, Carroll T, Taylor B, Terry A, Liang Z, Bruno L, Dharmalingam G, Khadayate S, Cobb BS, and Smale ST. 2013. Genome-wide identification of Ikaros targets elucidates its contribution to mouse B cell lineage specification and pre-B cell differentiation. Blood: blood-2012-2008-450114.
15. Sabbattini P, Lundgren M, Georgiou A, Chow C. m., Warnes G, and Dillon N. 2001. Binding of Ikaros to the λ5 promoter silences transcription through a mechanism that does not require heterochromatin formation. The EMBO Journal 20: 2812–2822. [PubMed: 11387214]
16. Thompson EC, Cobb BS, Sabbattini P, Meixlsperger S, Parelho V, Liberg D, Taylor B, Dillon N, Georgopoulos K, and Jumaa H. 2007. Ikaros DNA-binding proteins as integral components of B cell developmental-stage-specific regulatory circuits. Immunity 26: 335–344. [PubMed: 17363301]
17. Joshi I, Yoshida T, Jena N, Qi X, Zhang J, Van Etten RA, and Georgopoulos K. 2014. Loss of Ikaros DNA-binding function confers integrin-dependent survival on pre-B cells and progression to acute lymphoblastic leukemia. Nature immunology 15: 294. [PubMed: 24509510]
18. Macias-Garcia A, Heizmann B, Sellars M, Marchal P, Dali H, Pasquali J-L, Muller S, Kastner P, and Chan S. 2016. Ikaros is a negative regulator of B1 cell development and function. Journal of Biological Chemistry 291: 9073–9086.
19. Kuehn HS, Boisson B, Cunningham-Rundles C, Reichenbach J, Stray-Pedersen A, Gelfand EW, Maffucci P, Pierce KR, Abbott JK, and Voelkerding KV. 2016. Loss of B cells in patients with heterozygous mutations in IKAROS. New England Journal of Medicine 374: 1032–1043.
20. Hoshino A, Okada S, Yoshida K, Nishida N, Okuno Y, Ueno H, Yamashita M, Okano T, Tsumura M, and Nishimura S. 2017. Abnormal hematopoiesis and autoimmunity in human subjects with germline IKZF1 mutations. Journal of Allergy and Clinical Immunology 140: 223–231.
21. Ng SY-M, Yoshida T, and Georgopoulos K. 2007. Ikaros and chromatin regulation in early hematopoiesis. Current opinion in immunology 19: 116–122. [PubMed: 17307348]
22. Schjerven H, McLaughlin J, Arenzana TL, Frietze S, Cheng D, Wadsworth SE, Lawson GW, Bensinger SJ, Farnham PJ, and Witte ON. 2013. Selective regulation of lymphopoiesis and leukemogenesis by individual zinc fingers of Ikaros. Nature immunology 14: 1073–1083. [PubMed: 24013668]
23. Heizmann B, Kastner P, and Chan S. 2018. The Ikaros family in lymphocyte development. Current opinion in immunology 51: 14–23. [PubMed: 29278858]

24. Georgopoulos K, Bigby M, Wang J-H, Molnar A, Wu P, Winandy S, and Sharpe A. 1994. The Ikaros gene is required for the development of all lymphoid lineages. Cell 79: 143–156. [PubMed: 7923373]
25. Winandy S, Wu P, and Georgopoulos K. 1995. A dominant mutation in the Ikaros gene leads to rapid development of leukemia and lymphoma. Cell 83: 289–299. [PubMed: 7585946]
26. Schwickert TA, Tagoh H, Schindler K, Fischer M, Jaritz M, and Busslinger M. 2019. Ikaros prevents autoimmunity by controlling anergy and Toll-like receptor signaling in B cells. Nature immunology: 1–13.
27. Papathanasiou P, Perkins AC, Cobb BS, Ferrini R, Sridharan R, Hoyne GF, Nelms KA, Smale ST, and Goodnow CC. 2003. Widespread failure of hematolymphoid differentiation caused by a recessive niche-filling allele of the Ikaros transcription factor. Immunity 19: 131–144. [PubMed: 12871645]
28. Kirstetter P, Thomas M, Dierich A, Kastner P, and Chan S. 2002. Ikaros is critical for B cell differentiation and function. European journal of immunology 32: 720–730. [PubMed: 11870616]
29. Andrews TD, Whittle B, Field M, Balakishnan B, Zhang Y, Shao Y, Cho V, Kirk M, Singh M, and Xia Y. 2012. Massively parallel sequencing of the mouse exome to accurately identify rare, induced mutations: an immediate source for thousands of new mouse models. Open biology 2: 120061. [PubMed: 22724066]
30. Miosge LA, Field MA, Sontani Y, Cho V, Johnson S, Palkova A, Balakishnan B, Liang R, Zhang Y, and Lyon S. 2015. Comparison of predicted and actual consequences of missense mutations. Proceedings of the National Academy of Sciences 112: E5189–E5198.
31. Randall KL, Lambe T, Johnson A, Treanor B, Kucharska E, Domaschenz H, Whittle B, Tze LE, Enders A, and Crockford TL. 2009. Dock8 mutations cripple B cell immunological synapses, germinal centers and long-lived antibody production. Nature immunology 10: 1283–1291. [PubMed: 19898472]
32. McNamara HA, Idris AH, Sutton HJ, Vistein R, Flynn BJ, Cai Y, Wiehe K, Lyke KE, Chatterjee D, and Natasha K. 2020. Antibody feedback limits the expansion of B cell responses to malaria vaccination but drives diversification of the humoral response. Cell Host & Microbe 28: 572–585. e577. [PubMed: 32697938]
33. Ronni T, Payne KJ, Ho S, Bradley MN, Dorsam G, and Dovat S. 2007. Human Ikaros function in activated T cells is regulated by coordinated expression of its largest isoforms. J Biol Chem 282: 2538–2547. [PubMed: 17135265]
34. Patro R, Duggal G, Love MI, Irizarry RA, and Kingsford C. 2017. Salmon provides fast and bias-aware quantification of transcript expression. Nature methods 14: 417. [PubMed: 28263959]
35. Zerbino DR, Achuthan P, Akanni W, Amode MR, Barrell D, Bhai J, Billis K, Cummins C, Gall A, and Girón CG. 2017. Ensembl 2018. Nucleic acids research 46: D754–D761.
36. Team, R. C. 2013. R: A language and environment for statistical computing.
37. Soneson C, Love MI, and Robinson MD. 2015. Differential analyses for RNA-seq: transcript-level estimates improve gene-level inferences. F1000Research 4.
38. Love MI, Huber W, and Anders S. 2014. Moderated estimation of fold change and dispersion for RNA-seq data with DESeq2. Genome biology 15: 550. [PubMed: 25516281]
39. Kuznetsova A, Brockhoff PB, and Christensen RHB. 2017. lmerTest package: tests in linear mixed effects models. Journal of Statistical Software 82.
40. Morgan B, Sun L, Avitahl N, Andrikopoulos K, Ikeda T, Gonzales E, Wu P, Neben S, and Georgopoulos K. 1997. Aiolos, a lymphoid restricted transcription factor that interacts with Ikaros to regulate lymphocyte differentiation. The EMBO journal 16: 2004–2013. [PubMed: 9155026]
41. Kelley CM, Ikeda T, Koipally J, Avitahl N, Wu L, Georgopoulos K, and Morgan BA. 1998. Helios, a novel dimerization partner of Ikaros expressed in the earliest hematopoietic progenitors. Current Biology 8: 508–S501. [PubMed: 9560339]
42. Åkerfelt M, Morimoto RI, and Sistonen L. 2010. Heat shock factors: integrators of cell stress, development and lifespan. Nature reviews Molecular cell biology 11: 545. [PubMed: 20628411]
43. Jego G, Lanneau D, De Thonel A, Berthenet K, Hazoumé A, Droin N, Hamman A, Girodon F, Bellaye P, and Wettstein G. 2014. Dual regulation of SPI1/PU. 1 transcription factor by heat shock

factor 1 (HSF1) during macrophage differentiation of monocytes. Leukemia 28: 1676. [PubMed: 24504023]

44. Inouye S, Izu H, Takaki E, Suzuki H, Shirai M, Yokota Y, Ichikawa H, Fujimoto M, and Nakai A. 2004. Impaired IgG production in mice deficient for heat shock transcription factor 1. Journal of Biological Chemistry 279: 38701–38709.
45. Fernando TM, Marullo R, Gresely BP, Phillip JM, Yang SN, Lundell-Smith G, Torregroza I, Ahn H, Evans T, and Győrffy B. 2019. BCL6 evolved to enable stress tolerance in vertebrates and is broadly required by cancer cells to adapt to stress. Cancer discovery 9: 662–679. [PubMed: 30777872]
46. Baumjohann D, Preite S, Reboldi A, Ronchi F, Ansel KM, Lanzavecchia A, and Sallusto F. 2013. Persistent antigen and germinal center B cells sustain T follicular helper cell responses and phenotype. Immunity 38: 596–605. [PubMed: 23499493]
47. Boutboul D, Kuehn HS, Van de Wyngaert Z, Niemela JE, Callebaut I, Stoddard J, Lenoir C, Barlogis V, Farnarier C, and Vely F. 2018. Dominant-negative IKZF1 mutations cause a T, B, and myeloid cell combined immunodeficiency. The Journal of clinical investigation 128.
48. Ding Y, Zhang B, Payne JL, Song C, Ge Z, Gowda C, Iyer S, Dhanyamraju PK, Dorsam G, and Reeves ME. 2019. Ikaros tumor suppressor function includes induction of active enhancers and super-enhancers along with pioneering activity. Leukemia 33: 2720–2731. [PubMed: 31073152]
49. Karnowski A, Cao C, Matthias G, Carotta S, Corcoran LM, Martensson I-L, Skok JA, and Matthias P. 2008. Silencing and nuclear repositioning of the λ5 gene locus at the pre-B cell stage requires Aiolos and OBF-1. PLoS One 3: e3568. [PubMed: 18974788]
50. Wang J-H, Avitahl N, Cariappa A, Friedrich C, Ikeda T, Renold A, Andrikopoulos K, Liang L, Pillai S, and Morgan BA. 1998. Aiolos regulates B cell activation and maturation to effector state. Immunity 9: 543–553. [PubMed: 9806640]
51. Vairy S, and Tran TH. 2020. IKZF1 alterations in acute lymphoblastic leukemia: The good, the bad and the ugly. Blood Reviews: 100677. [PubMed: 32245541]
52. Nunes-Santos CJ, Kuehn HS, and Rosenzweig SD. 2020. IKAROS Family Zinc Finger 1–Associated Diseases in Primary Immunodeficiency Patients. Immunology and Allergy Clinics 40: 461–470.

Key points

IKAROS ZF1 is crucial for normal development and function of B cells but not T cells.

The L132P mutation in IKAROS confers a CVID-like phenotype in mice.

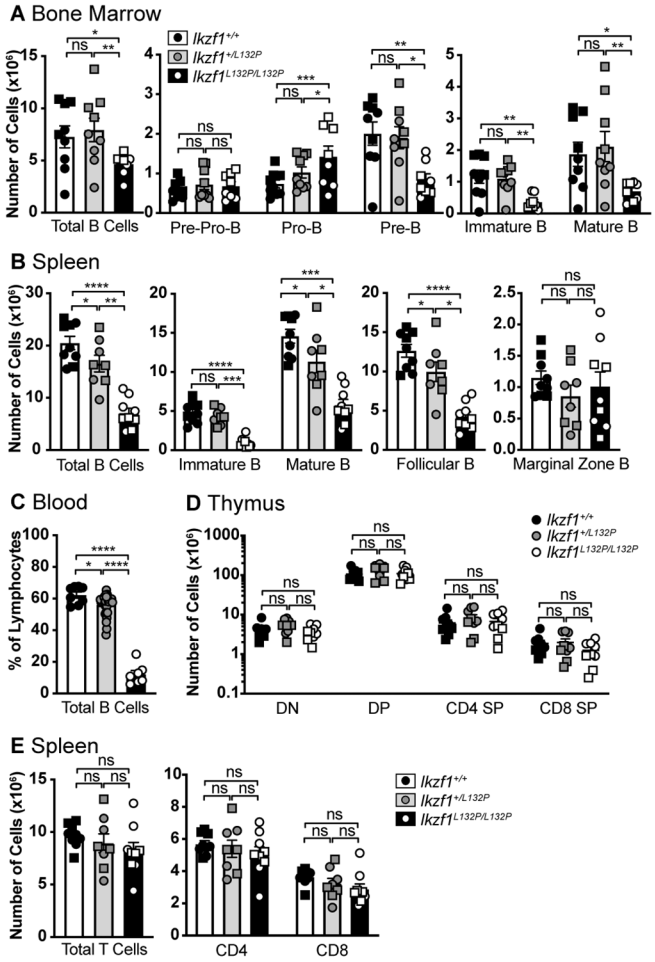

Figure 1. L132P mutation affects B cell, but not T cell development in mice.

Effect of L132P mutation on B cell (A-B) and T cell (C-D) development determined by flow cytometry. (A) B cell development in the bone marrow. (B) B cell subsets in the spleen. (C) Frequency of B cells in the peripheral blood. (D) T cell development in the thymus. (E) T cell subsets in the spleen. (A-E) Columns represent the mean of each group ± SEM, individual mice represented by a symbol, (A, B, D, E) data pooled from two independent experiments with circles and squares differentiating the two experiments, n=8-9 per group. (C) Data pooled from five independent experiments, n= 7-31 per group. (A-E) One-way, pairwise ANOVA with multiple comparison assuming equal standard variation. Independent experiments used as blocking factor in R to determine significance. DN, double negative; DP, double positive; SP, single positive.

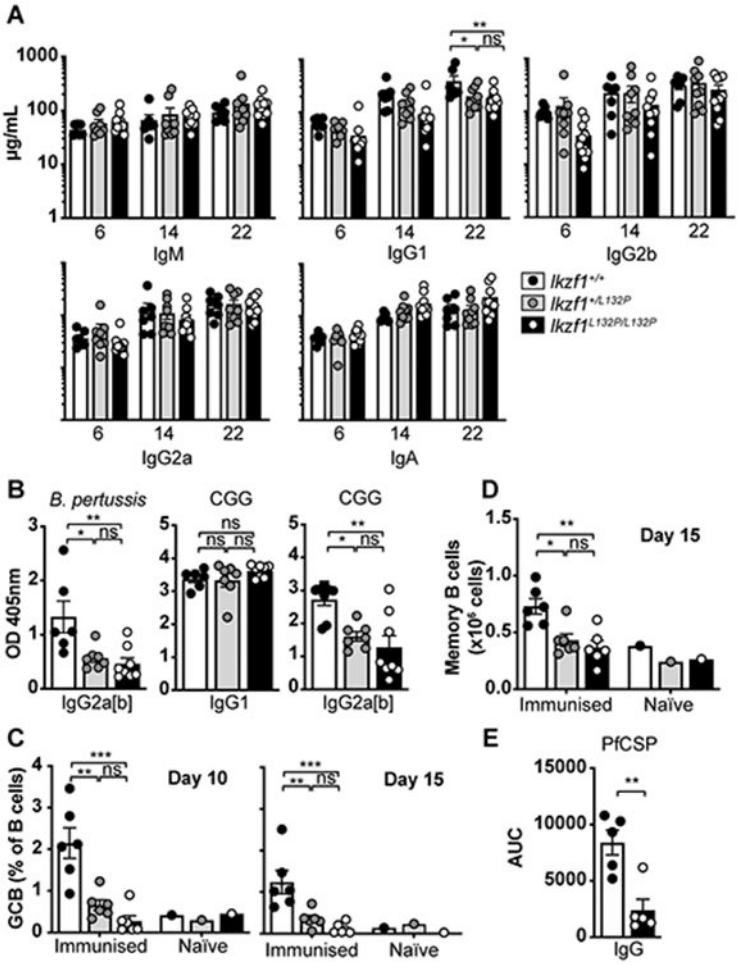

Figure 2. Reduced humoral immune response in heterozygous and homozygous mice.

(A) Concentration of different subtypes of secreted immunoglobulins in plasma of naïve mice over time, determined by Meso scale assay system, n=7-11 per group. (B) Optical density (OD) of antigen-specific antibodies measured in plasma collected 2 weeks after immunization with *B. pertussis* and chicken-gamma-globulin (CGG) in Alum, n=6-8 per group. (C) Percent of germinal center B cells (GCB) in the spleen 10 and 15 days after immunization with sheep red blood cells (SRBCs), determined by flow cytometry. (D) Number of memory B cells in the spleen 15 days post immunization with SRBCs. (E) Area under curve (AUC) from ELISA of *P. falciparum* circumsporozoite protein (PfCSP)-specific IgG in the serum 5 days post booster immunization with PfCSP in Alum. (A-E) Columns represent the mean of each group ± SEM, individual mice represented by individual symbols. Data from one experiment. (A-D) One-way, pairwise ANOVA with multiple comparisons assuming equal standard variation. (E) Student's unpaired T test.

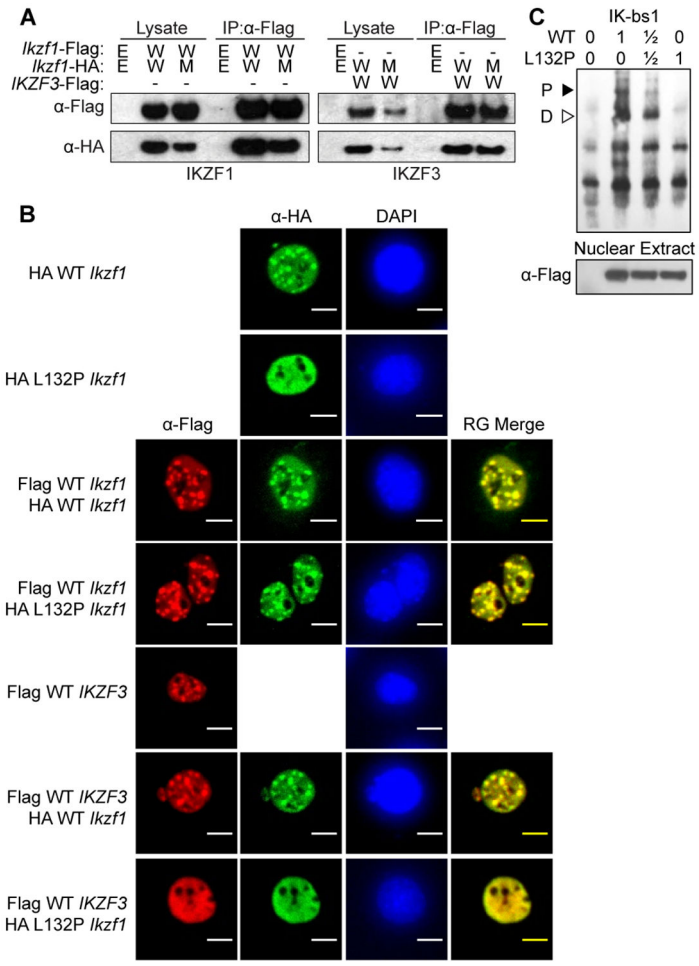

Figure 3. L132P mutant IKZF1 maintains dimerization abilities but is unable to localize to pericentromeric heterochromatin and bind target DNA sequences.

(A) Co-immunoprecipitation of HEK293T cells; HEK293T cells were co-transfected with either Flag-tagged wildtype (W) *Ikzf1* (pFlag CMV2-Ikzf1 WT) and HA-tagged WT or L132P mutant (M) *Ikzf1* (pcDNA3.1-HA-WT or L132P) or Flag and HA empty vectors (E) (left panels). In addition, HEK293T cells co-transfected with either Flag WT *IKZF3* (pcDNA3.1-DYK-IKZF3) and HA WT *Ikzf1*, Flag WT *Ikzf3* and HA L132P mutant *Ikzf1*, or Flag and HA empty vectors. Immunoprecipitation (IP) performed with anti-Flag antibody and western blot performed on pull-down products using anti-Flag and anti-HA antibodies. 10% total protein lysate used as loading/protein expression control. Data representative of three independent experiments. (B) Immunofluorescence showing pericentromeric-heterochromatin localization. NIH3T3 cells transfected with HA-tagged WT or L132P mutant *Ikzf1* (top 2 rows), or co-transfected with Flag WT and HA WT *Ikzf1*, or Flag WT and HA L132P mutant *Ikzf1* (3rd and 4th rows). NIH3T3 cells transfected with Flag-tagged WT *IKZF3*, or co-transfected with Flag WT *IKZF3* and HA WT *Ikzf1*, or Flag WT *IKZF3* and HA L132P mutant *Ikzf1* (bottom 3 rows). Cells seeded onto coverslips and stained with anti-Flag and anti-HA monoclonal antibodies followed by Alexa594 (red) and Alexa488-conjugated (green) secondary antibodies and DAPI nuclear staining. Cells visualized using a ZOE fluorescent cell imager (Bio-Rad, Original magnification 175x) and then cropped and

merged after acquisition using ImageJ software. Data representative of at least five cells per condition and two independent experiments. Scale bar = 10μm. (C) Electrophoretic mobility shift assay (EMSA) of HEK293T cells transfected with either pFlag-CMV2-WT or L132P mutant *Ikzf1*, or a 1:1 ratio of WT and L132P mutant *Ikzf1*. Nuclear fraction of cell lysate incubated with either biotinylated IK-bs1 DNA binding sequences and DNA/protein complexes detected using HRP-conjugated streptavidin. Arrows indicate bands corresponding to IKZF1 multimerization with DNA probes; P: polymer, D: dimer. Nuclear extracts western blotted for IKZF1 expression as a loading control (bottom panel). Data representative of 3 independent experiments.

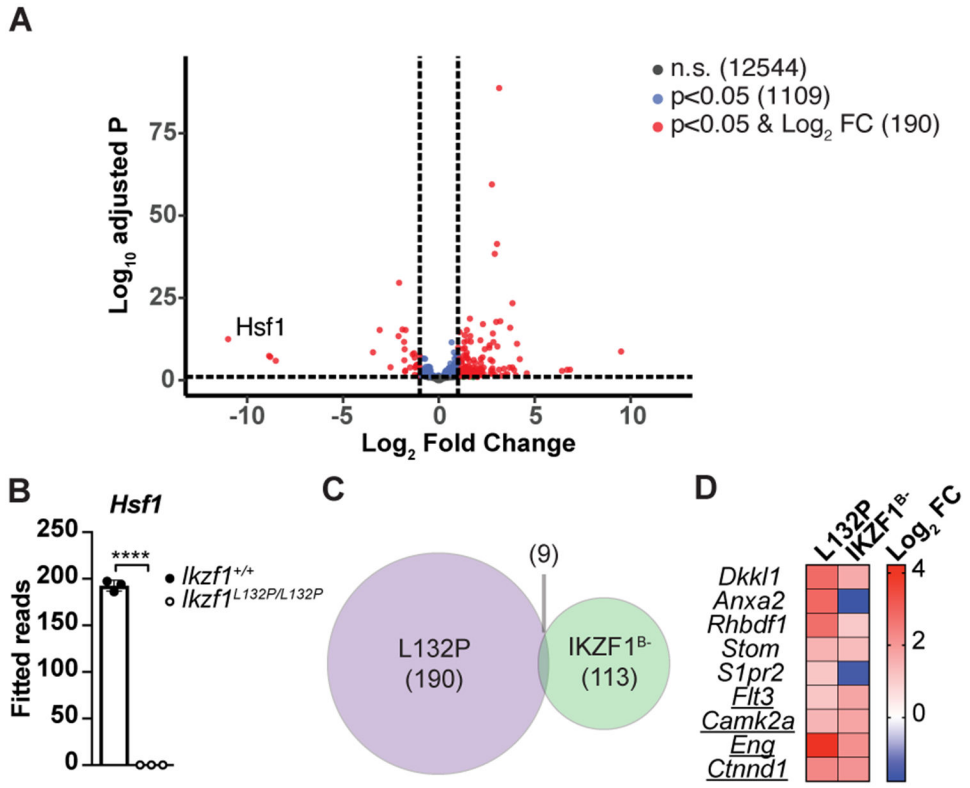

Figure 4. *Ikzf1*$^{L132P/L132P}$ follicular B cells have a unique gene signature including a complete absence of *Hsf1* expression.

(A) Volcano plot of gene expression in *Ikzf1*$^{L132P/L132P}$ FoB cells compared to wildtype, defined as genes with a greater than four-fold difference and adjusted P value of <0.05 (red dots), or genes with an adjusted P value of <0.05 (blue dots), or non-significant genes (grey dots). (B) Expression of *Hsf1* in FoB cells measured by RNAseq. Columns show the mean for each group ± SEM, mice represented by individual dots, n=3. Unpaired two-tailed T test. (C) Venn diagram of genes differentially expressed in *Ikzf1*$^{L132P/L132P}$ (L132P) FoB compared with genes differentially expressed in *Ikzf1*$^{B-}$ FoB cells (26) showing the overlap of genes that are significantly different in both data sets determined by RNAseq. (D) Average $\log_2$ fold change of genes differentially expressed in both L132P and B cell conditional knock-out of *Ikzf1* (IKZF1^{B-}) mice (26) compared to controls. Underlined genes have been shown to be directly bound by IKZF1 (26). (A-D) *Ikzf1*$^{+/+}$ n=3, *Ikzf1*$^{L132P/L132P}$ n=3. (C-D) *Ikzf1*$^{B+}$ n=2, *Ikzf1*$^{B-}$ n=2.